

Surface modification of sized vegetal fibers through direct fluorination for eco-composites

Olivier Teraube^{a,b,*}, Jean-Charles Agopian^{a,b}, Elodie Petit^a, François Metz^c, Nicolas Batisse^a, Karine Charlet^b, Marc Dubois^a

^a Université Clermont Auvergne, SIGMA Clermont, ICCF, BP 10448, 63000 Clermont-Ferrand, France

^b Université Clermont Auvergne, SIGMA Clermont, Institut Pascal, BP 10448, 63000 Clermont-Ferrand, France

^c Solvay SpecialChem, 85 avenue des Frères Perret, 69192 SAINT-FONS Cedex, France

* Corresponding author at : Université Clermont Auvergne, SIGMA Clermont, ICCF, BP 10448, 63000 Clermont-Ferrand, France

E-mail address: olivier.teraube@uca.fr (O. Teraube)

Telephone number : +33613668908

Abstract

Natural fibers are frequently used as alternatives of glass fibers as polymer matrix reinforcement to form composite materials. However, their natural hydrophilicity prevents them from being easily compatible with hydrophobic polymers, which represent the majority of matrices. To solve this, direct fluorination of sized natural fibers (flax fibers sized with DGEBA) was performed. EDX, FTIR and ¹⁹F NMR analysis evidenced the chemical grafting of fluorine on DGEBA structure and the ablation of the oxiranes rings on this molecule. Chemical modifications of DGEBA have induced a hydrophobic character of this layer, by reducing at 0 the polar component of surface tension. Thereby, treated fibers are supposed to be perfectly chemically compatible with the hydrophobic polymer matrices (*e.g.* polypropylene). Additionally, the fluorination time also allows the dispersive component of surface tension and the rugosity of fibers to be tailored in order to perfectly adjust these characteristics and fit with the polymer. Moreover, this chemical modification was achieved without altering the mechanical properties of fibers for short fluorination times.

Keywords: Natural fiber; DGEBA; Fluorination; Eco-composite; Compatibilization; Hydrophobicity.

1 Introduction

Vegetal fibers are materials produced and recycled naturally for millions of years. These fibers are more and more used as alternatives of glass fibers for polymer matrices reinforcement to form composites materials [1–5]. Indeed, those compounds allow to develop natural, local and renewable resources while lightening the cost and the overall weight of these materials, thanks to the specific properties of natural fibers, equivalent to glass fibers one. This specificity provides them to be frequently used in the automotive and aeronautical industry [1,4,6]. Besides, their use is more environmentally friendly than using synthetic fiber (like glass, carbon or aramid) and therefore, fits perfectly with the environmental issue of the XXIst century. Indeed, using natural fibers with a biodegradable and/or biobased polymer matrix allows “eco-composite” with a low environmental footprint to be prepared.

Despite this, one of the main difficulties in the use of these compounds as composite reinforcement is their hydrophilicity. Indeed, vegetal fibers are mainly composed of cellulose, lignin, and hemicelluloses which have a large number of hydroxyl and carboxyl groups in their chemical structure that provides to lignocellulosic fibers a high polarity with a polar component of surface tension γ_s^p of 26,0 mN/m (and a dispersive component γ_s^d of 34 mN/m) [7]. To obtain good filler/matrix interfacial properties, both materials must have close polar and dispersive components of surface tension. However, polymer matrices are mainly hydrophobic, with a very low γ_s^p (Table I). Consequently, most of the time, a poor interfacial adhesion is created between polymer matrix and vegetal fibers which leads to a decrease of the global mechanical performance of the composite [8–11]

Polymer		γ_s (mN/m)	γ_s^d (mN/m)	γ_s^p (mN/m)	Reference
<i>Biobased Biodegradable</i>	<i>Poly(lactic acid (PLA)</i>	41.6	30.8	10.8	[12]
	<i>poly(β-hydroxybutyrate) (PHB)</i>	34.3	22.8	11.5	[13]
<i>(Potentially) Biobased Non Biodegradable</i>	<i>Polyethylene (PE)</i>	35.3- 35.7	35.3- 35.7	0	[14]
	<i>Polyisobutylene (PB)</i>	33.6	33.6	0	[14]
	<i>Polyamide 66 (PA 66)</i>	47	40.8	6.2	[15]
	<i>Polypropylene (PP)</i>	30.1	30.1	0	[14]
<i>Non Biobased Biodegradable</i>	<i>Polycaprolactone (PCL)</i>	30.8	26.1	4.7	[16]
<i>Other polymer matrices</i>	<i>Epoxy “E11”</i>	51.6	32.6	19	[17]
	<i>Poly(etheretherketone) (PEEK)</i>	44.8	43.4	1.4	[18]

Table I - Surface tension component of different polymers

In order to reduce the polar component of natural fiber surface tension, many different methods have been developed. As examples, corona treatment,

torrefaction, acetylation, malleated coupling, mercerization, and peroxide treatments may be cited as well as a lot of other chemical and/or physical processes [19–24]. However, these processes are unfortunately costly, both time and energy consuming and may degrade the fibers (and the mechanical properties in the same way), and/or harmful to the environment and people by using toxic solvents. Another methods consist to carry out a chemical grafting on the fiber surface to provide good compatibility with a hydrophobic polymer (e.g. Polypropylene which is one of the most popular composite matrices). One of the representative examples of this technique is the use of maleic anhydride-grafted polypropylene (MAPP) to create a chemical “bridge” between fibers (natural or artificial) or the fiber sizing [25–27]. However, once again these methods generally use dangerous substances e.g. maleic anhydride, which is dangerous for operators’ respiratory organs.

In that context, we propose to use direct fluorination to counter the hydrophilic behavior of natural fibers. Indeed, a chemical treatment under molecular fluorine F_2 would result in a covalent grafting of fluorine atoms located at the outmost surface if the process is perfectly controlled [28–30]; such a chemical treatment provides hydrophobic properties to the material. This process may be performed at the industrial scale as exemplified by the fluorination of the petrol car tank that significantly increases its barrier properties [31]. In addition, this method is a quick and low energy consuming reaction, which occurs spontaneously at room temperature with most of the polymers; vacuum or electric field is not necessary. Furthermore, fluorination is also an industrial process, so there is a possibility to up-scale this treatment in the future. Finally, once perfectly controlled fluorination has a very low environmental footprint, which is a good point to make “eco-friendly” materials and allows to treat fibers without any human contact with the reactant.

If direct fluorination could be directly employed on lignocellulosic materials (e.g. wood, wood flour, etc.) [28,32–34], we propose in this study to investigate its effect on the fiber sizing. The idea is to add a hydrophobic character to the surface of fiber via the sizing without reducing the chemical affinity of the sizing polymer with fibers. The controlled fluorination is expected to increase the mechanical properties and the water-resistance of composite materials by the use of a treatment which is more respectful of the environment than those already existing.

2 Experimental

2.1 Fluorination

Fluorination of sized natural fibers was performed inside a passivated nickel reactor (covered with NiF_2) in dynamic conditions (under a continuous flux of gases in an opened reactor). Sized flax fiber samples were pieces of tissue whose dimensions are $2.5 \times 4 \text{ cm}^2$, which have been cut from a uni-directional FlaxPly tissue, sized with “an epoxy polymer” and purchase from Eco-Technilin. The reactive gas consists of a mixture of pure fluorine, purchased from Solvay Fluor (less than 0.1 vol.% of admixtures, mainly oxygen), and pure Nitrogen (99,999 % purity). Before each reaction, fibers were outgassed during 1h under primary vacuum (10^{-3} mbar) at 80°C , and the reactor was flushed for 1h with nitrogen gas to remove all traces of air and moisture. Then, fibers were exposed to a reactive flow of F_2 / N_2 (in a 1:1 volume ratio). The flow rate of each gas was 20mL/min and reactions were performed at room temperature during 1min, 2min 30s, 5 min, 7min 30s, 10min, 15min and 20 min. Once the fluorination process was achieved, fluorine flow was stopped and the

reactor was flushed again with pure nitrogen gas (80 mL/min) for 1h to stop the reaction and eliminate traces of F_2 , HF , CF_4 , and C_2F_6 (those gases were removed by a soda-lime trap). Finally, the fibers were once again outgassed for 1 hour under primary vacuum (10^{-3} mbar) at $80^\circ C$ to remove all fluorine-based gases from the sample surface.

2.2 Characterizations

FTIR experiments were carried out with a Nicolet 6700 FT-IR (Thermo Scientific) spectrometer in ATR mode. For each spectrum, 32 scans with 4 cm^{-1} resolution were collected between 4000 and 524 cm^{-1} .

1H and ^{13}C NMR spectrum were carried out on liquid phase with a 400 MHz Bruker Avance spectrometer. All those experiments were performed in $CDCl_3$.

^{19}F solid state NMR experiments were performed using a 300 MHz Bruker Avance spectrometer. A magic-angle spinning (MAS) probe operating with 2.5 mm rotors was used allowing a 30 kHz spinning rate. For ^{19}F MAS spectra, a simple sequence was used with a single $\pi/2$ pulse duration of $4.0\ \mu s$. ^{19}F chemical shifts were externally referenced to CF_3COOH and then referenced to $CFCl_3$ ($\delta_{CF_3COOH} = -78.5\text{ ppm}$ vs δ_{CFCl_3})

To measure the glass transition of fiber sizing, Differential Scanning Calorimetry (DSC) was used. Experimentation was performed under a flow rate of 20 mL/min of nitrogen gas, from 193K to 373K with a heat flow of 10K/min.

To investigate on the morphological impact of the fluorination, samples were observed using a scanning electron microscope (SEM). During those investigations, the energy of the electron beam was 3KeV and for each sample, pictures were captured at 2000x of magnification. In addition, the measure of the fluorine percentage present inside the fluorinated sample was performed using a XFlash - Quantax EDS detector for SEM.

To evaluate the impact of the treatment on the surface tension of compound, contact angle measurements were performed using a AM4113ZT Dino-Lite handheld digital microscope. Because of the shape of fibers, it is not possible to use "standard" sessile drop technique. According to Schellbach and al. [35], it is possible to measure the contact angle between a liquid and a fiber by filling a drop of liquid between 2 fibers and measuring the distance between those fibers and the height of the formed meniscus. This method was performed using 4 different liquids (Water, Formamide, Ethylene glycol, and Diiodomethane) and the contact angle between those liquid and the fiber was calculated (with at least 6 measurements per sample, taken at different locations). After that, the polar and dispersive components of the surface tension of each sample were obtained using Owens and Wendt's method [36].

In addition, the average absorption time was measured; a drop of water was deposited on the fibers. Then the absorption of water by the tissue was filmed using an Attension Theta Lite Optical Tensiometer in a $19^\circ C$ temperature-controlled room and constant 33% of relative humidity. The absorption speed was obtained from the time needed by the sample to absorb a drop of water and the measure of water drop size thanks to ImageJ software. In addition, to consider the evaporation phenomenon, the same experimentation was performed on a sample of PTFE (which does not absorb water). Thereby, the absorption speed was corrected with the evaporation component. Finally, the time to absorb a 5mm^3 water drop was calculated. For each sample, 3 measures were systematically performed. Furthermore, contact angle of molten polyethylene onto fibers was performed by

positioning a drop of molten polyethylene onto fiber surface. This molten PE is obtained at 150°C for about 10 minutes. The fibers with molten PE drop was quickly removed from the oven. Thereby, the drop freezes and can be observed with an Attension Theta Lite Optical Tensiometer to measure the angle.

Surface roughness of sample was measured by atomic force microscopy (AFM). Experiments were carried out using a Bruker Innova® Atomic Force Microscope equipped with a 12nm radius silicone probe. For each sample, a surface of 1.5µm x 1.5µm was scanned in 512 lines, in tapping mode with resonant frequency of 0.3 Hz.

The change of the mechanical properties (Young's modulus (E), Ultimate tensile strength (σ_m) and maximal elongation percentage (% ϵ)) was investigated via tensile tests of fluorinated (or not) sized flax yarn. For each sample, at least 15 wires are glued on different paper frames, according to [37]. Their diameter was estimated from the average of 3 microscopes measurements (100x of magnification). Then, tensile test was carried out using an Instron 5543 devices equipped with a 50N load cell. During experimentations, the gauge length was 10 mm and the crosshead displacement rate was constant at 1 mm/min, up to rupture. Finally, the different properties (E, σ_m , % ϵ) were calculated according to the NF T25-501-2 standard.

2.3 Sizing extraction

2.3.1 Protocol

Approximately 5g of sized fibers were placed into a 250mL conical flask and covered with ethanol for 7 days (the color of the liquid turned from translucent to light yellow). Then, the liquid was heated until most of the ethanol was removed. The final brown viscous substance was recuperated for identification.

2.3.2 Spectroscopic and thermal data

2-[[4-[2-[4-(oxiran-2-ylmethoxy)phenyl]propan-2-yl]phenoxy]methyl]oxirane; oil; FT-IR : 3500 (v-OH), 3050(v-C-H oxirane ring),2965-2961(v-C-H aliphatic), 1604 + 1510 + 1452 (v-C=C aromatic), 1226(v-C-O oxirane), 1030 (v-C-O ether), 913(v-C-O oxirane), 828(v-C-O-C oxirane), 770(γ -CH₂); ¹H NMR (CDCl₃): 7.15 (d,4H, J= 9.2 Hz), 6.83 (d, 4H, J= 8.6 Hz), 4.20 (dd, 2H, J= 3.1, 11.2 Hz), 3.95 (dd, 2H, J= 5.5, 11.2 Hz), 3.32–3.35 (m, 2H),2.89 (dd = t, 2H, J= 4.3 Hz), 2.74 (dd, 2H, J= 2.6, 4.9 Hz),1.63 (s, 6H); (3.70, q +1.24, t = Ethanol); ¹³C NMR (CDCl₃): d 156.2 (C), 143.7 (C),127.7 (CH), 114.0 (CH), 68.7 (CH₂), 50.2 (CH), 44.8(CH₂), 41.7 (C), 31.0 (CH₃); (58.3 (CH₂) + 18.4 (CH₃) = Ethanol).

DSC : Tg onset = -22°C ; Tg endset = -3 °C;

3 Results and discussion

3.1 Sizing identification

The structure of extracted sizing polymer has been analyzed by FT-IR spectroscopy, DSC, ¹H and ¹³C NMR. Results (*c.f.* part 2.3.2) fit perfectly with DGEBA matrix analysis presented in the literature (FT-IR [38–41], NMR: [38,38,40,42,43] and DSC [40,44]). Moreover, the fact that the sizing is composed of DGEBA also matches with commercial information provided by the provider (Eco-Technilin) who announces that flax fibers are sized with an epoxy polymer. The chemical structure of DGEBA is presented in Fig. 1.

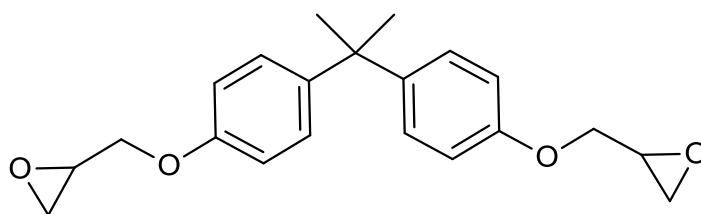


Fig. 1: DGEBA chemical structure

3.2 Presence of fluorine

EDX and FT-IR analysis have been performed on fluorinated samples. EDX results (Fig. 2) showed the presence of fluorine atoms whatever the sample. In addition, results showed that the percentage of fluorine was increasing with the fluorination duration (with the highest fluorine content for 15min of fluorination). This indicates that the fluorinated layer is the thickest and/or the more dense for 15 min of fluorination.

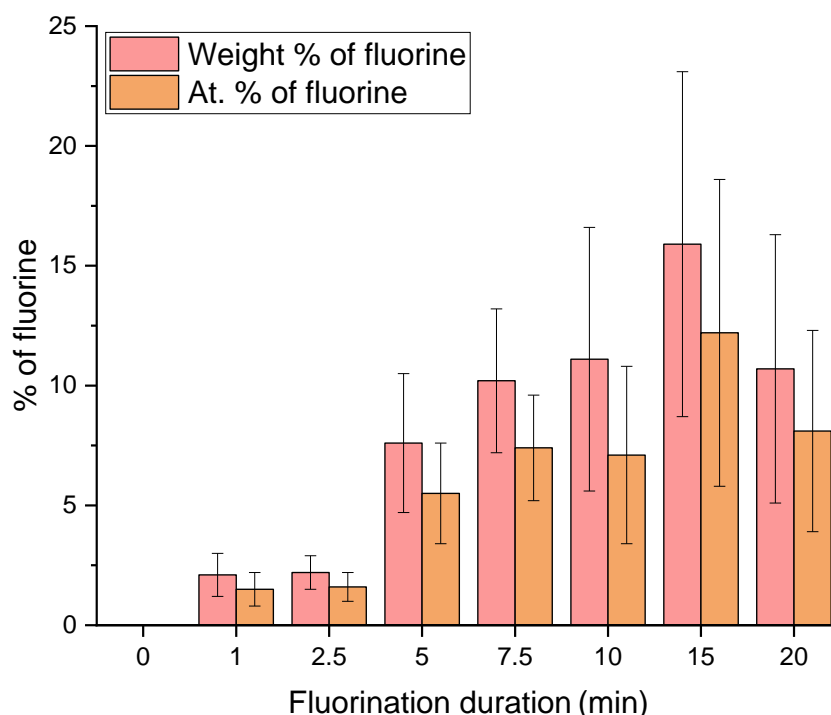


Fig. 2: Fluorine At. and weight % vs. fluorination duration obtained by EDX analysis

Moreover, covalent grafting of fluorine is proved by the evolution of the IR spectra. Indeed, the deconvolution of IR data shows the appearance of several carbon-fluorine vibration bands between 800 and 1800 cm^{-1} , on the IR spectra (red lines in Fig. 3). This evidenced the creation of covalent C-F bonds.

Furthermore, evolutions on the spectra show the disappearance of several peaks (purple lines in Fig. 3), and particularly at 1500 cm^{-1} . This particular vibration band is assigned to the aromatic rings of the DGEBA [39], and its extinction reveals the disappearance of this group from the chemical structure during the fluorination. Several other peaks, which correspond to C-H bond (and maybe C-C bond too) disappeared or decreased in intensity. However, the apparition of peaks assigned to C-F bonds complicates the analysis and the understanding of the reaction mechanism of DGEBA fluorination with IR spectroscopy.

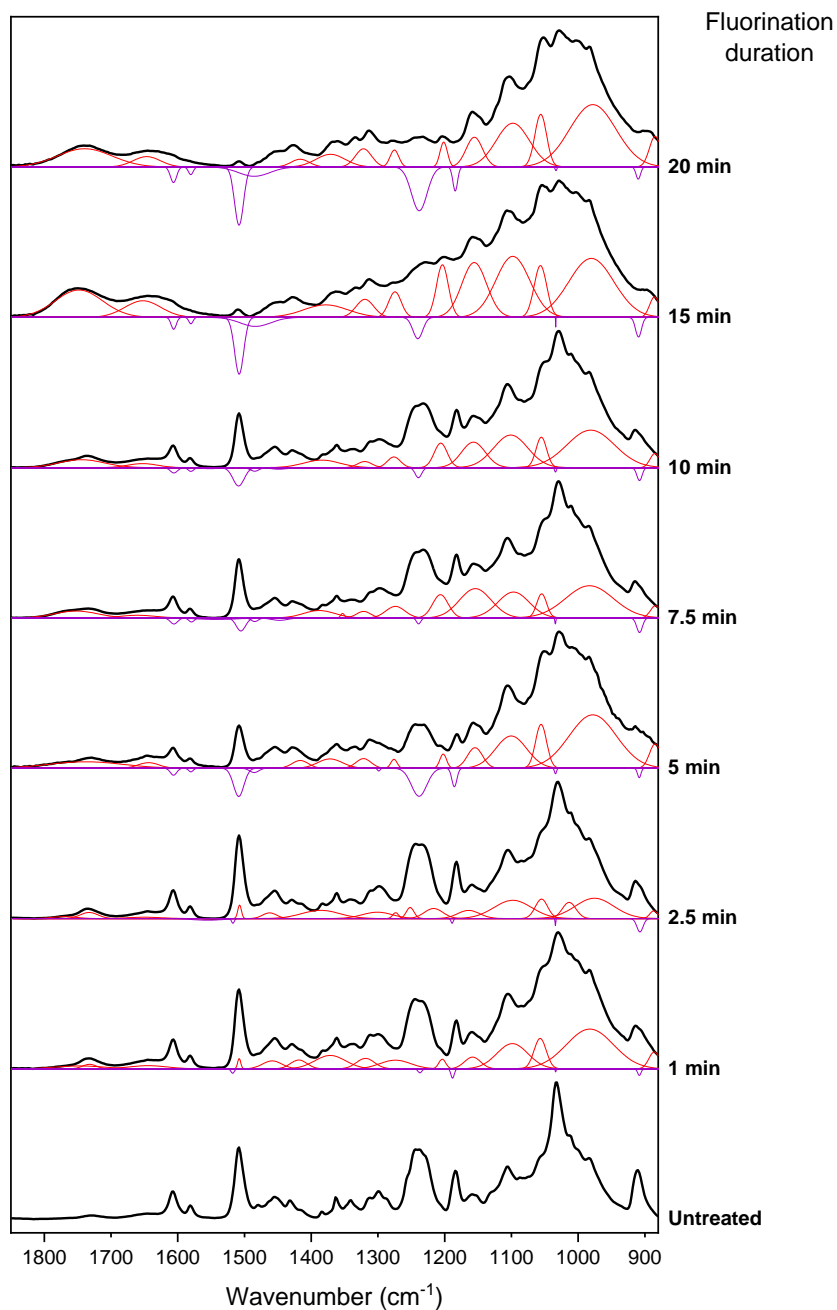


Fig. 3: FT-IR spectra of raw and fluorinated sized flax fibers

3.3 Fluorination Mechanism

In order to better understand the sizing fluorination mechanism, solid state ^{19}F NMR experimentations were carried out, and the results are shown in Fig. 4. It is recognized that polymer fluorination mainly transforms CH_x groups in CF_3 , CF_2 or CH_yF groups [45,46]. Chemical shifts of these three groups are respectively between -40/-90 ppm, -100/-155 ppm, -160/-250 ppm (highlighted with a grey background in Fig. 4). Most of the time, CF_2 groups correspond to the perfluorination of carbon (which means the carbon only makes bonds with fluorine(s) and other carbon(s)) and CF_3 groups result from the disruption of the C-C skeleton. Thereby, a first analysis of these spectra evidences no (or weak) degradation for 1min and 2min 30s of fluorination. Then, between 5 and 10 min of fluorination, a moderated degradation takes place and higher degradation rates are reached for 15 and 20 min of fluorination.

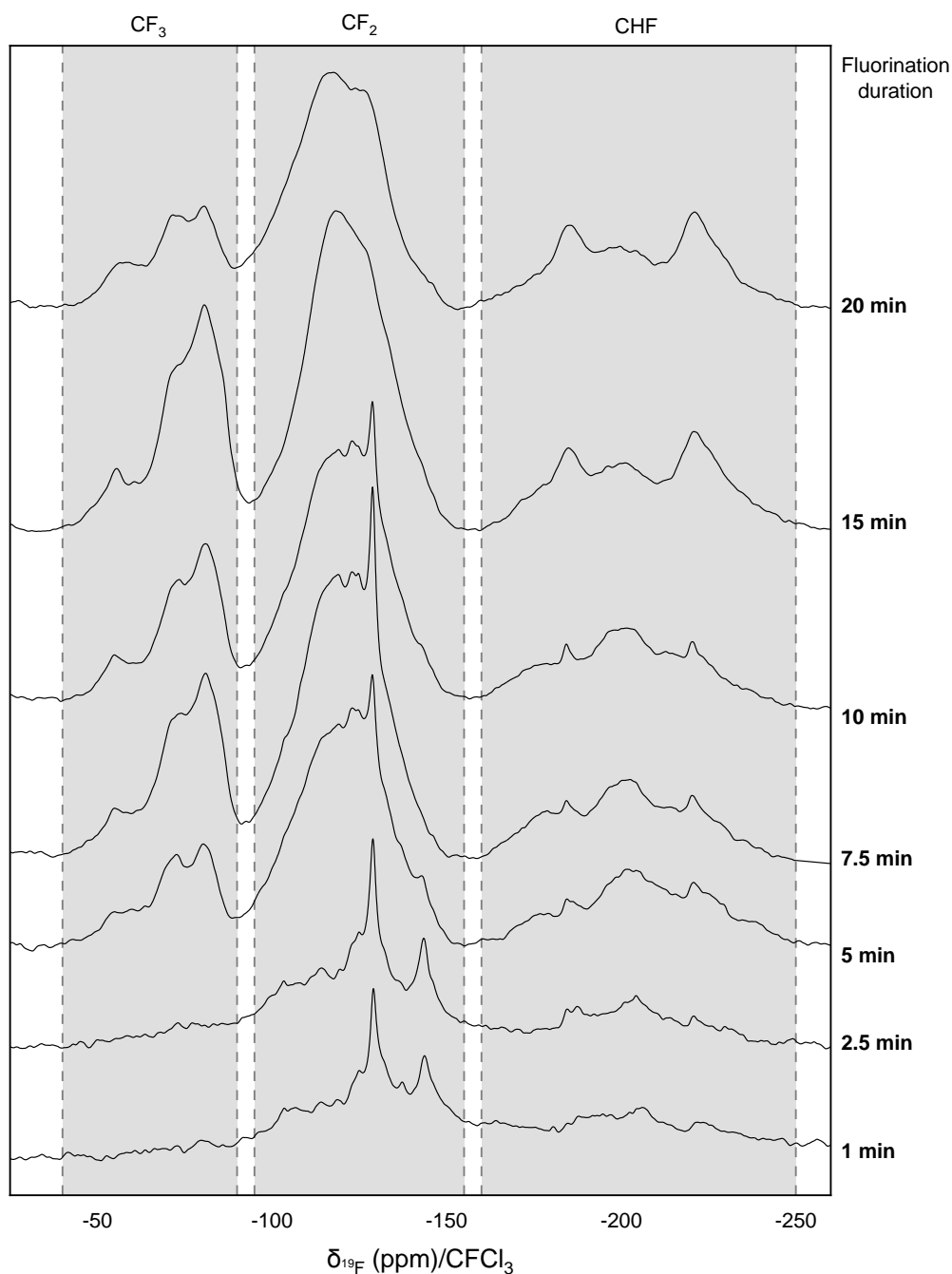
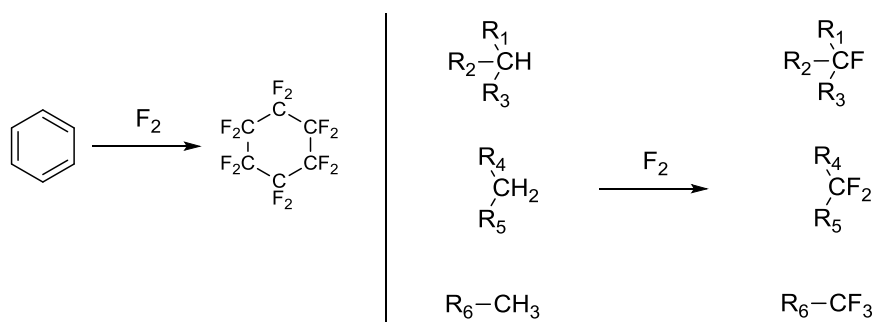


Fig. 4: ^{19}F solid-state NMR spectrum of fluorinated sized fibers

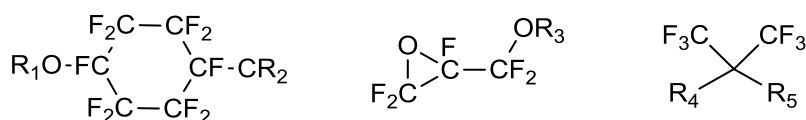
The narrowness of lines for shortest fluorination rates is explained by dilution of F atoms. The ^{19}F - ^{19}F homonuclear dipolar coupling is lowest that for longer treatment. Such interaction results in a broadening of the components which are numerous according to the number of F atoms in the neighboring (e.g. $\text{CF}_2\text{-CFH-CF}_2$, CHF-CFH-CF_2 , CHF-CFH-CHF , $\text{CH}_2\text{-CFH-CH}_2\text{...}$)

To go deeper into data exploitations, some previous works on polymer fluorination may be considered. In 1979, Lagow & Margrave [45] have shown the perfluorination of aromatic ring and CH_x group leads to the following reactions (Scheme 1) :

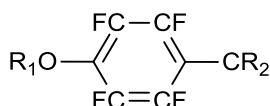


Scheme 1 : Perfluorination mechanism of aromatic ring and CH_x group, according to Lagow & Margrave [45]

Consequently, by analogy, perfluorination of DGEBA may form the following chemical groups:



In addition to this point, Kharitonov's works [46,47] showed perfluorination does not happen instantly, and kinetics of this reaction is different for all chemical groups. Consequently, following group may appear during the fluorination process, in addition to CH_xF_y :



At this step, it is possible to identify most of the ^{19}F NMR chemical shifts of all these chemical groups but not all since the literature does not give precisely these data. Indeed, CF_x groups are reported that have a chemical environment close to those we are studying. Considering that fluorine environment deshields fluorine nuclei, because of the very high electronegativity of this atom (3.98 on Pauling scale [48]), possible assignments of chemical shifts for DGEBA's perfluorinated group are presented in Table II.

However, as discussed previously, an over-fluorination (step after perfluorination) result in a disruption of the main carbon chain. Thanks to this observation, it is possible to plan which groups are likely to form (Fig. 5). However, considering the internal tension of the oxirane ring, the high reactivity of the aromatic ring, and the high stability of the C_6F_{10} ring, some species are less likely to form; underlined with a grey background in Fig. 5. Their expected chemical shifts are added in Table II.

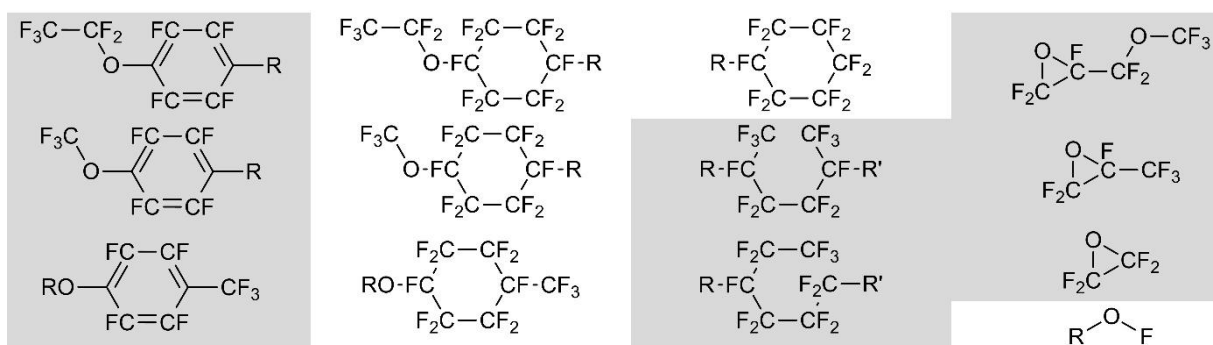
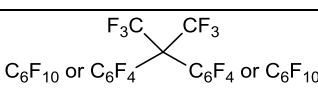
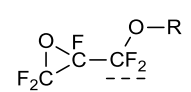
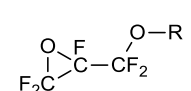
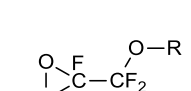
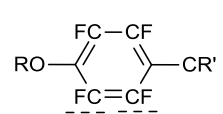
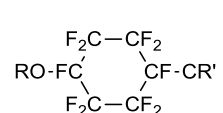
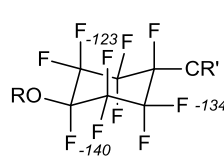

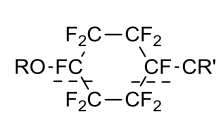
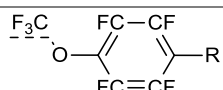
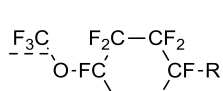
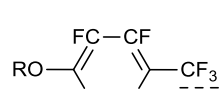
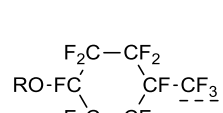
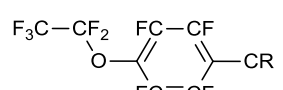


Fig. 5 : Potential over-fluorinated groups of DGEBA

Perfluorinated groups

Chemical group	$\delta_{\text{Theoretical}}$ (ppm)	δ_{Spectrum} (ppm)
	> -59 [44]	-55
	~ -80 [49]	-80
	-111 and -115 ; [50]	-114 -119
	~ -158 [50]	-164
	-141 and -161 [51]	-143 -156
		-124 -129 -137
	[52-54]	-143 -185
	[52-54]	-143 -185

Over-fluorinated groups

	> -58 [50]	-55
	~ 55 [52]	-55
	-62 [50]	-63
	~ -70 [53,54]	-73
	> -88 [55]	-81

$\begin{array}{c} \text{F}_3\text{C}-\text{CF}_2 \quad \text{F}_2\text{C}-\text{CF}_2 \\ \diagdown \quad \diagup \\ \text{O}-\text{FC} \quad \text{CF}-\text{CR} \\ \diagup \quad \diagdown \\ \text{F}_2\text{C}-\text{CF}_2 \end{array}$	> -88 [50]	-81
$\begin{array}{c} \text{F}_2\text{C}-\text{CF}_2 \\ \diagdown \quad \diagup \\ \text{R}-\text{FC} \quad \text{CF}_2 \\ \diagup \quad \diagdown \\ \text{F}_2\text{C}-\text{CF}_2 \end{array}$	-125, -143 [52-54]	-124, -143
$\begin{array}{c} \text{F}_3\text{C} \quad \text{CF}_3 \\ \diagdown \quad \diagup \\ \text{R}-\text{FC} \quad \text{CF}-\text{R}' \\ \diagup \quad \diagdown \\ \text{F}_2\text{C}-\text{CF}_2 \end{array}$		
+		
$\begin{array}{c} \text{F}_2\text{C}-\text{CF}_3 \\ \diagdown \quad \diagup \\ \text{R}-\text{FC} \quad \text{F}_2\text{C}-\text{R}' \\ \diagup \quad \diagdown \\ \text{F}_2\text{C}-\text{CF}_2 \end{array}$	~-80 [56]	-80
$\begin{array}{c} \text{O} \quad \text{F} \quad \text{O}-\text{CF}_3 \\ \diagdown \quad \diagup \quad \diagdown \\ \text{F}_2\text{C}-\text{C}-\text{CF}_2 \end{array}$	-55 [57]	-55
$\begin{array}{c} \text{O} \quad \text{F} \\ \diagdown \quad \diagup \\ \text{F}_2\text{C}-\text{C}-\text{CF}_3 \end{array}$	-78 [50]	-80
$\begin{array}{c} \text{O} \\ \diagdown \quad \diagup \\ \text{F}_2\text{C}-\text{C}-\text{CF}_2 \end{array}$	-111 [58]	-111
$\text{R}-\text{O}-\text{F}$	> +120 [59]	∅

Table II - Chemicals shifts of perfluorinated and overfluorinated groups of DGEBA

By comparing theoretical NMR shifts and the solid-state ^{19}F NMR results, it is possible to go further on the fluorination mechanism of DGEBA (presented on Scheme 2). In a first time, it is possible to claim that the chemical group (A) (Table III) is formed because of the presence of its corresponding peaks at -156 ppm (and -143 ppm) for short fluorination. In addition, results evidence that the perfluorinated molecule (Fig. 6) is readily formed, because of the presence of the corresponding peaks of this molecule (Table II) from 1 min of fluorination.

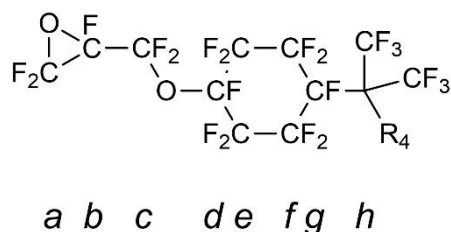


Fig. 6 : Perfluorinated DGEBA

This underlines the high reactivity of DGEBA. However, all positions have not the same reactivity towards fluorine gas. On the perfluorinated molecule (Fig. 6), two privileged sites of rupture have been identified:

i- The first one is the site labelled *b* (on Fig. 6). Indeed, the quick disappearance of the -164 ppm band which corresponds to the CF group of the oxirane group (B) (Table III) attests that this position is very reactive, quickly over fluorinated, resulting the loss of the oxirane group (after 2min 30s of fluorination for our samples).

ii- The second one is the *h* position. Indeed, the high intensity of the -73 ppm peak proved (C) compound (Table III), is significantly formed, indicating the carbon between the two rings is another privileged place of rupture. In addition the low intensity of the band at -55 ppm indicates that CF₃ on *h* position (Fig. 6) would exhibit a very high reactivity and then readily form gaseous CF₄.

Results also evidence that *a*, *e* and *f* positions (Fig. 6) are favorably formed and very stable (not likely over-fluorinated) and showed there is only 4 chemical over-fluorinated groups (Scheme 2) which are mainly formed (other over-fluorinated groups may be formed, but they will be in minority).

The main features are discussed here and detailed NMR analysis are provided in the supporting information.

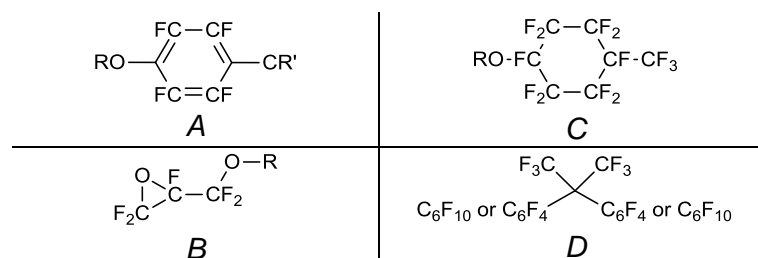
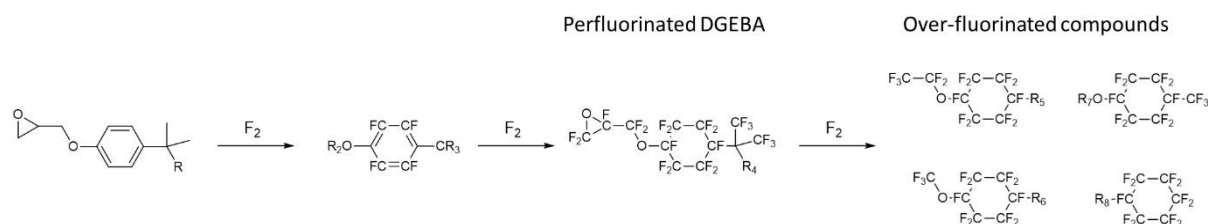


Table III - Fluorinated species expected during the fluorination

Thereby, direct fluorination mechanism between F₂ and DGEBA sizing is summarized in Scheme 2. This reaction occurs by a multi-step mechanism which leads in a first time to perfluorination of DGEBA. Presence of the chemical group (A) (Table III) evidences that fluorine react on aromatic ring through an addition reaction, as already observed and described by Luo *et al.*[60] on benzene rings of aramid fiber treated by direct fluorination. At the same time (but according to different kinetics and reactivity) CH_x group react with F₂ in order to form CH_yF_z groups in a first time, and CF_x groups ultimately. These reaction leads to the formation of perfluorinated DGEBA (Fig. 6). However, if the reaction is not stopped, DGEBA will further react with fluorine, generating disruptions on different places of this molecule, mainly close to oxygen atom and cycle, as presented on Scheme 2.



Scheme 2: Direct fluorination mechanism of DGEBA

3.4 Impact of fluorination

3.4.1 Surface tension

As demonstrated previously, in addition to grafting fluorine on the molecule, fluorination also quickly removes the oxirane ring, responsible for hydrophilic properties of DGEBA. These two chemical modifications have an important impact on the surface tension of fluorinated sized fibers. Indeed, in Fig. 7a are represented polar (γ_s^p), dispersive (γ_s^d) and total (γ_s) surface tension of fluorinated sized fibers. On the one hand, from 1 min to 10 min of fluorination, γ_s^p is close to 0. This means the polar character is suppressed from the sizing surface for these fluorination

durations. On the other hand, we notice that the dispersive component evolved at the same time. Indeed, between 1 and 5 min, γ_s^d decreases and then, from 7min 30s to 10 min, γ_s^d increases. This phenomenon, already observed on direct fluorination of wood [32], evidence that this treatment decreases the dispersive component of surface tension, for short time of fluorination. Beyond this time, γ_s^d starts to increase, probably because of the degradation phenomenon.

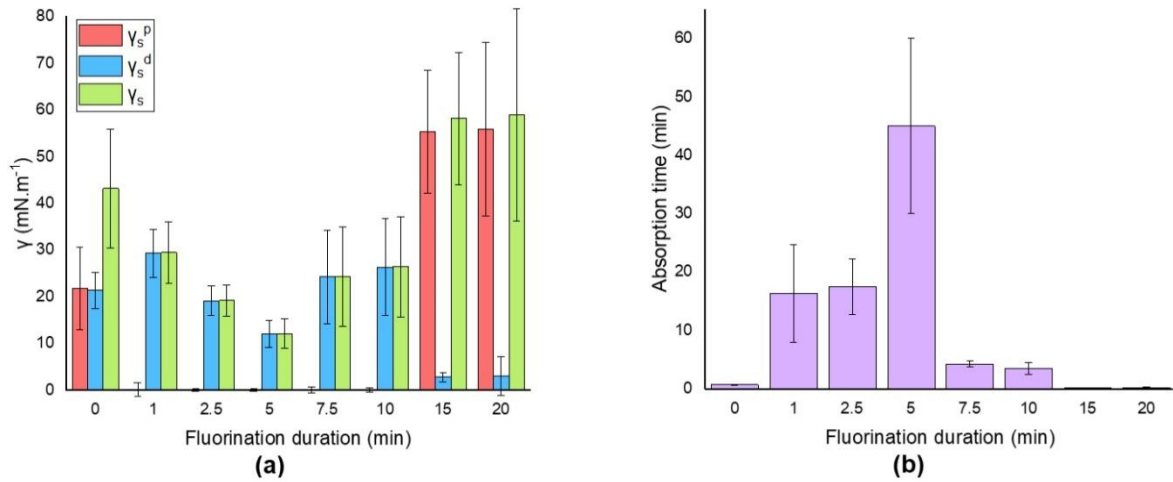


Fig. 7 : (a) Polar, dispersive and total surface energy of fluorinated sized fibers; (b) Average absorption time of a 5mm^3 water drop by sized fluorinated fibers

To have the best interfacial adhesion, polymer matrix and fillers must have the closest γ_s^p and γ_s^d . By comparing the fluorinated DGEBA components with those ones of other polymer matrix (Table I), it is possible to evaluate the interfacial affinity considering the two components. Thereby, fluorinated DGEBA onto fibers exhibits enhanced affinity. For example, when the surface tensions of 1min fluorinated fibers and raw fibers are compared to the values of polyethylene or polypropylene (which are the most common ones to make composites). Fibers covered with fluorinated sizing match perfectly with PP and PE matrix (Table IV), that suggests improved adhesion in the composite. In order to prove that fact, contact angle of PE, molten at 150°C onto fibers has been measured (Fig. 8). Results show an important decrease of the contact angle after fluorination treatment, evidencing the compatibilization of fluorinated fibers with PE (and more widely, with all hydrophobic polymers). It must be noted that, to perform the measurement, molten PE drop should be added at 150°C onto fibers. Then, the whole is transferred at room temperature (to observe the angle), resulting in solidification of the PE. During this change of state, a slight shrinkage may occur, which would slightly modify (positively or negatively) the contact angle. Nevertheless, this phenomenon cannot explain the significant difference of contact angles between untreated and fluorinated fibers, then mainly due to the compatibilization of fluorinated fibers with hydrophobic polymers. Moreover, Maity *et al.*, in their works on aramid and UHMWPE fibers reinforced high density polyethylene and low density polyethylene, respectively [61,62]; have demonstrated that fluorination of fibers allows to increase mechanical properties of composites by increasing composite's adhesion between fiber and PE-matrix. Additionally, this treatment also improved the thermal stability and the wetting properties of composite.

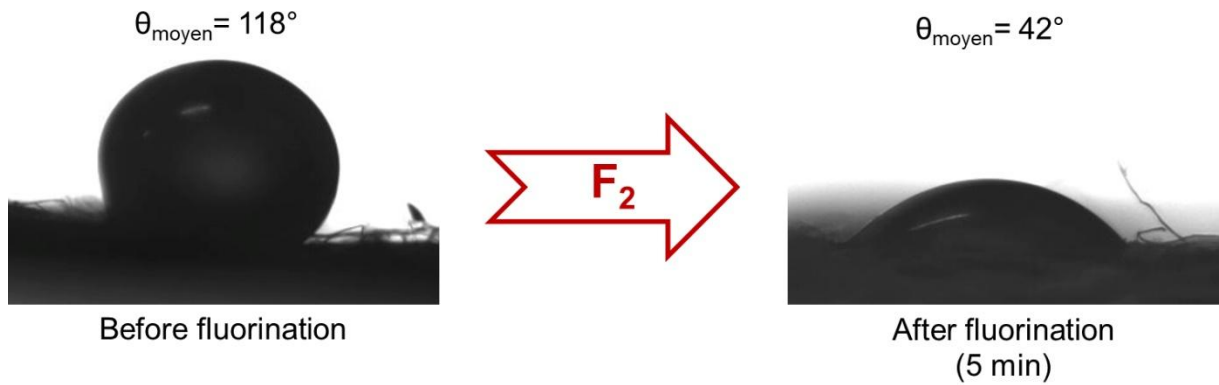


Fig. 8 : Impact of fluorination on contact angle between liquid PE and fibers

Additionally, by controlling the fluorination duration, the tailoring of the dispersive component may be achieved in order to perfectly fit with polymer matrices. Thereby, if PHB is selected as a polymer matrix ($\gamma_s^d = 22.8$ mN/m) instead of PP, an increase in fluorination duration from 1 to 2 min 30s (for our sample) would allow to perfectly fit with this other polymer. Those two examples evidence the versatility of the surface chemistry thanks to fluorination;

Also, water absorption time is significantly increased as shown in Fig. 7b. This point is particularly interesting to ensure a good viability of the composite materials by decreasing the water absorption/desorption of the vegetal fibers, that usually generates cracks into the material [10].

	γ_s^d (mN/m)	γ_s^p (mN/m)
Raw fibers	21.4	21.8
1 min fluorinated fibers	29.3	0.2
2.5 min fluorinated fibers	19.2	0
Polypropylene (PP)	30.1	0
Polyethylene (PE)	35.3-37.7	0
Poly(β -hydroxybutyrate) (PHB)	22.8	11.5

Table IV - Comparison of raw fibers, fluorinated fibers and different matrices surface tension components

3.4.2 Surface roughness

Another surface characteristic modified by direct fluorination is roughness, by the fact that F_2 has an etching effect on the surface of organic materials [63,64]. This point will favor the fiber/matrix mechanical anchoring and improve by another way the mechanical properties of the final composite. In order to observe this phenomenon, SEM pictures (Fig. 9) and AFM experiments (Fig. 10) have been recorded.

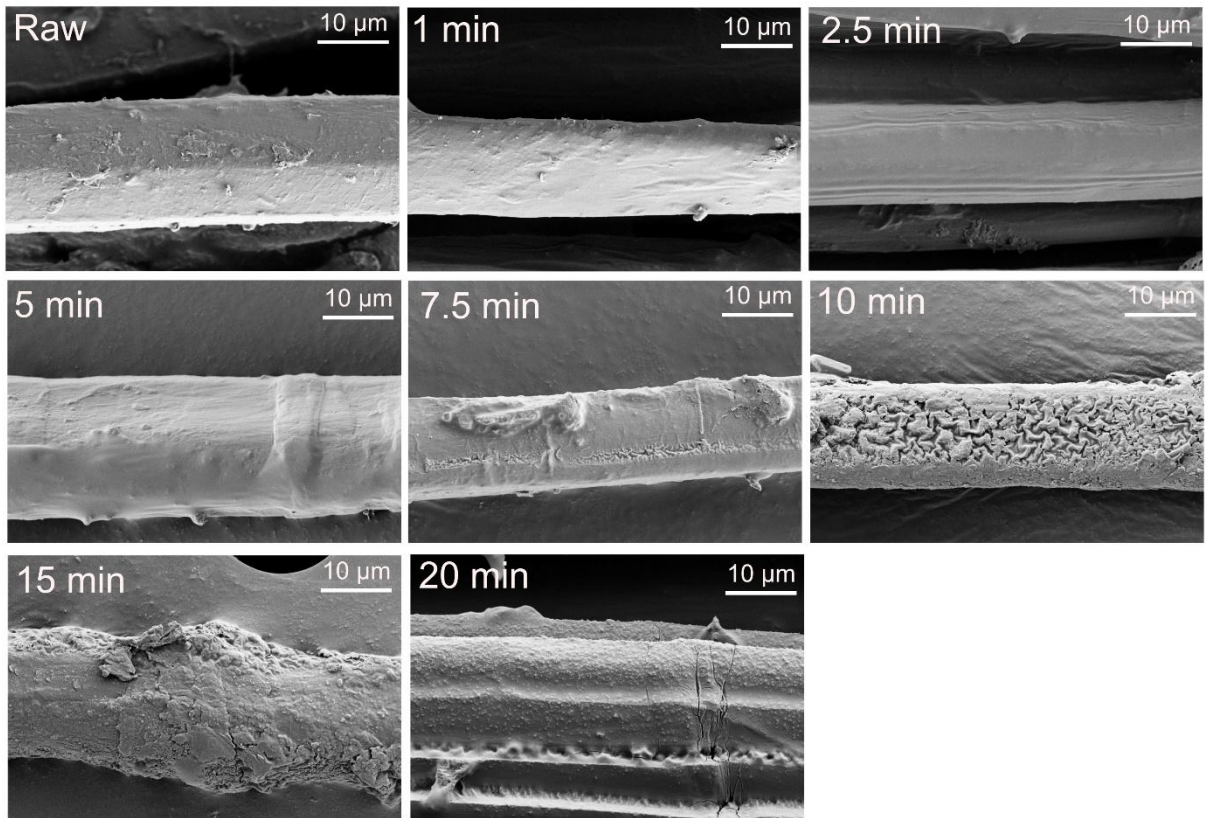


Fig. 9: SEM photography of raw and fluorinated sized fibers

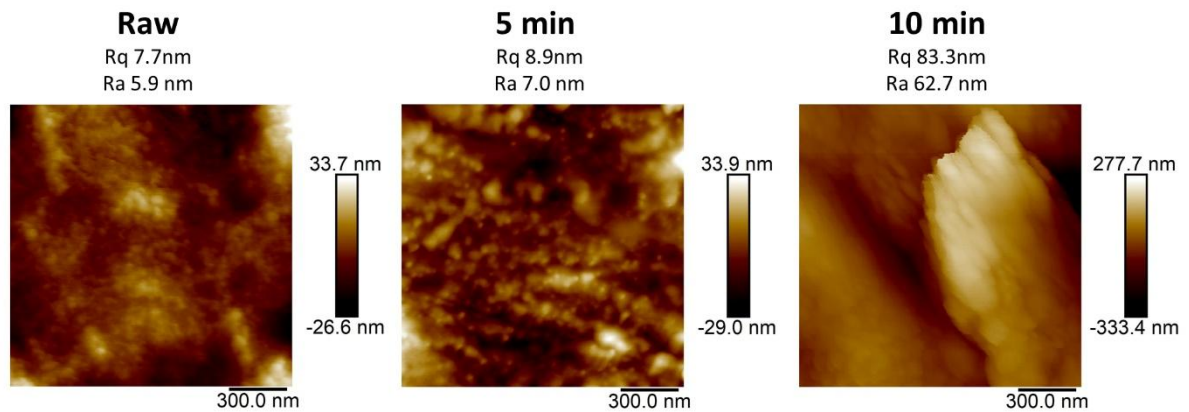


Fig. 10: AFM images of raw and fluorinated sized fibers

Thereby, from 1 to 5 min, no significant modifications appears on SEM pictures. AFM data of the 5 min fluorinated fibers and the raw one evidence a small increase of the mean surface roughness (Rq and Ra). This means that short time fluorination induced nano-scale etching, which is expected to act on wettability of fibers, because of fakir effect [65]. Dispersive component is then changed, see Fig. 7a. Moreover, this phenomenon increases the number of anchor points, and consequently, the fibers/matrix interface strength. After 5 min of fluorination, degradation of fibers begins, in accordance with the presence of the band related to CF_3 groups on ^{19}F NMR spectra (Fig. 4). This phenomenon results also in cracks on the fiber surface as seen by SEM images (Fig. 9), that consequently increases the surface roughness (Rq = 83nm and Ra = 63nm after 10min of fluorination). However, at these fluorination time, a micro-scale etching occurs in relation with the increase of

the surface tension from 7.5min of fluorination due to dispersive component (Fig. 7). After 10min of fluorination, SEM pictures show the loss of fiber sizing. Thereby, fiber parts emerge and only small sizing points still remain at the fiber surface. This phenomenon results in a significant increase of the polar component γ_s^d of fibers (Fig. 7a), because of the fact that natural fibers now contribute to the surface chemistry, giving back high hydrophilic properties to the materials.

To sum up, sizing fluorination occurs as presented on the schematic diagram Fig. 11

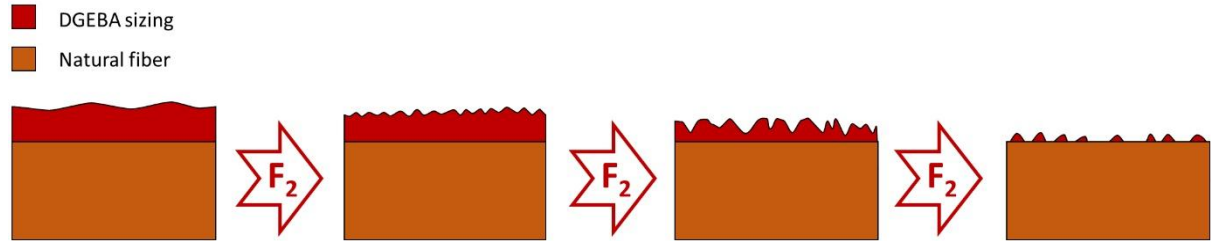


Fig. 11: Schematic diagram of fluorination impact on surface roughness

2.4.2 Mechanical properties

The tensile properties are showed in Fig. 12. Before discussing the results, considerations about the uncertainties of these experiments must be given. In Fig. 12, error bars, *i.e.* the standard deviations of the results, are relatively high (close to 25-30%); these significant variations come from the variability of natural fibers [66]. Indeed, the experimental uncertainty of Young's modulus can be obtained thanks to the following calculations :

$$E = \sigma/\varepsilon = F/S \times l_0/\Delta l = F/\Delta l \times 4/\pi \times l_0/d^2 \quad (1)$$

where σ is the strength at rupture in Pa, ε the strain at rupture in mm/mm, F the maximal tensile load applied in N, Δl the fiber length in m, l_0 the gauge length in m, S the fiber section in m^2 , and d the diameter in m.

In equation (1), the part $\frac{F}{\Delta l} \cdot \frac{4}{\pi}$ is composed of device parameters and constants. Consequently, this part of the equation is constant, and we will use the letter k to replace it. Thereby, (1) could be write as following (2)

$$E = k \times l_0/d^2 \quad (2)$$

Experimental uncertainties can be expressed by derivation of the equation (2) :

$$\Delta E/E = \Delta l_0/l_0 + 2\Delta d/d \quad (3)$$

By comparing the mean standard deviations of 27% and the mean experimental uncertainties of 5%, one may conclude that experimental uncertainties are significantly lower than the standard deviations. This means that the gap does not come from the experiment but rather from the materials.

The tensile test results evidence that the Young's modulus is constant with increasing fluorination duration. However, a decrease of both the ultimate tensile strength and the elongation is observed from 7min 30s to 20min of fluorination. This is in agreement with the fact that fluorination only affects the surface of samples. Indeed, Young's modulus reflects volume properties whereas ultimate tensile strength and maximum of elongation are more related to surface properties. In addition, the present results demonstrate that mechanical properties are not affected by a controlled fluorination (less than 5min in our experimental conditions). However, when this reaction is prolonged, properties at rupture (like ultimate tensile strength or maximum of elongation) start to be degraded.

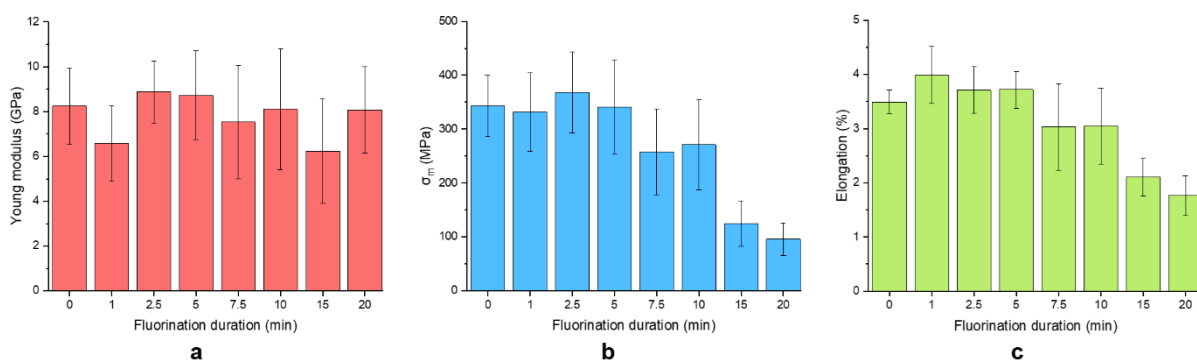


Fig. 12 : Evolution of the fiber mechanical properties with the fiber fluorination duration: (a) Young's modulus; (b) Ultimate tensile strength; (c) % of maximal elongation

4 Conclusion

Direct fluorination with F_2 gas of sized flax fibers (sizing with DGEBA) was performed. When controlled by a dilution with an inert gas (N_2) and short duration, this treatment converts the outmost surface of the sizing into a fluorinated polymer layer. ^{19}F NMR data evidence the fluorination of DGEBA *via* a covalent grafting of fluorine atoms as well as the fast loss of the oxirane ring which is responsible of the hydrophilicity of DGEBA but also compatibility with epoxy matrices. Those chemical modifications induced a significant decrease of the polar component of surface tension and allows fluorinated DGEBA layer to be compatible with hydrophobic polymers, e.g. polyethylene or polypropylene. In addition, the dispersive component of surface tension could be adjusted to perfectly fit with the chosen polymer thanks to a chemically tailored sizing. The fiber/sizing interface is not deteriorated because of the surface location of the controlled fluorination. In addition, fluorination duration allows the dispersive component of surface tension to be tailored as a function of polymer matrix chosen to be the matrix composite. Fluorination does not affect the mechanical properties of fibers, for a short treatment duration.

Acknowledgments

This work was financially supported by the Région Auvergne-Rhône-Alpes through the FLUONAT Project, and encouraged by Solvay Group.

References

- [1] J.S. Dhaliwal, Natural Fibers: Applications, in: M. Abbas, H.-Y. Jeon (Eds.), *Generation, Development and Modifications of Natural Fibers*, IntechOpen, 2019. <https://doi.org/10.5772/intechopen.86884>.
- [2] K. Charlet, *Contribution à l'étude de composites unidirectionnels renforcés par des fibres de lin : relation entre la microstructure de la fibre et ses propriétés mécaniques*, Thèse en chimie des matériaux, Université de Caen, 2006.
- [3] A. Moudood, A. Rahman, A. Öchsner, M. Islam, G. Francucci, Flax fiber and its composites: An overview of water and moisture absorption impact on their performance, *J. Reinf. Plast. Compos.* 38 (2019) 323–339. <https://doi.org/10.1177/0731684418818893>.
- [4] J. Holbery, D. Houston, Natural-fiber-reinforced polymer composites in automotive applications, *JOM.* 58 (2006) 80–86. <https://doi.org/10.1007/s11837-006-0234-2>.
- [5] C.-M. Wu, W.-Y. Lai, C.-Y. Wang, Effects of Surface Modification on the Mechanical Properties of Flax/ β -Polypropylene Composites, *Materials.* 9 (2016) 314–324. <https://doi.org/10.3390/ma9050314>.
- [6] P. Wambua, J. Ivens, I. Verpoest, Natural fibres: can they replace glass in fibre reinforced plastics?, *Compos. Sci. Technol.* 63 (2003) 1259–1264. [https://doi.org/10.1016/S0266-3538\(03\)00096-4](https://doi.org/10.1016/S0266-3538(03)00096-4).
- [7] M.F. Pucci, P.-J. Liotier, D. Seveno, C. Fuentes, A. Van Vuure, S. Drapier, Wetting and swelling property modifications of elementary flax fibres and their effects on the Liquid Composite Molding process, *Compos. Part A: Appl. Sci. Manuf.* 97 (2017) 31–40. <https://doi.org/10.1016/j.compositesa.2017.02.028>.
- [8] A. Céline, S. Fréour, F. Jacquemin, P. Casari, The hygroscopic behavior of plant fibers: a review, *Front. Chem.* 1 (2014) 1–12. <https://doi.org/10.3389/fchem.2013.00043>.
- [9] F.M. AL-Oqla, M.S. Salit, Natural fiber composites, in: *Materials Selection for Natural Fiber Composites*, Elsevier, 2017: pp. 23–48. <https://doi.org/10.1016/B978-0-08-100958-1.00002-5>.
- [10] H. Dhakal, Z. Zhang, M. Richardson, Effect of water absorption on the mechanical properties of hemp fibre reinforced unsaturated polyester composites, *Compos. Sci. Technol.* 67 (2007) 1674–1683. <https://doi.org/10.1016/j.compscitech.2006.06.019>.
- [11] V.K. Thakur, M. Thakur, M.R. Kessler, *Handbook of Composites from Renewable Materials*, Scrivener Publishing LLC, 2017.
- [12] O. Yousefzade, J. Jeddi, E. Vazirinasab, H. Garmabi, Poly(lactic acid) phase transitions in the presence of nano calcium carbonate: Opposing effect of nanofiller on static and dynamic measurements, *J. Thermoplast. Compos. Mater.* 32 (2019) 312–327. <https://doi.org/10.1177/0892705718759386>.
- [13] S. Zhang, X. Sun, Z. Ren, H. Li, S. Yan, The development of a bilayer structure of poly(propylene carbonate)/poly(3-hydroxybutyrate) blends from the demixed melt, *Phys. Chem. Chem. Phys.* 17 (2015) 32225–32231. <https://doi.org/10.1039/C5CP06076A>.
- [14] D.W. van Krevelen, K. te Nijenhuis, *Properties of polymers: their correlation with chemical structure: their numerical estimation and prediction from additive group contributions*, 4th, completely revised edition ed., Elsevier, Amsterdam, 2009.
- [15] J.E. Mark, *Polymer Data Handbook*, Oxford University Press, Inc., 1999.

- [16] L. Lins, V. Bugatti, S. Livi, G. Gorrasi, Ionic Liquid as Surfactant Agent of Hydrotalcite: Influence on the Final Properties of Polycaprolactone Matrix, *Polymers*. 10 (2018) 44–55. <https://doi.org/10.3390/polym10010044>.
- [17] E. Occhiello, M. Morra, G. Morini, F. Garbassi, D. Johnson, On oxygen plasma-treated polypropylene interfaces with air, water, and epoxy resins. II. Epoxy resins, *J. Appl. Polym. Sci.* 42 (1991) 2045–2052. <https://doi.org/10.1002/app.1991.070420732>.
- [18] A. Wilson, I. Jones, F. Salamat-Zadeh, J.F. Watts, Laser surface modification of poly(etheretherketone) to enhance surface free energy, wettability and adhesion, *Int J Adhes Adhes.* 62 (2015) 69–77. <https://doi.org/10.1016/j.ijadhadh.2015.06.005>.
- [19] A. Paul, K. Joseph, S. Thomas, Effect of surface treatments on the electrical properties of low-density polyethylene composites reinforced with short sisal fibers, *Compos. Sci. Technol.* 57 (1997) 67–79. [https://doi.org/10.1016/S0266-3538\(96\)00109-1](https://doi.org/10.1016/S0266-3538(96)00109-1).
- [20] A. Ali, K. Shaker, Y. Nawab, M. Jabbar, T. Hussain, J. Militky, V. Baheti, Hydrophobic treatment of natural fibers and their composites—A review, *J. Ind. Text.* 47 (2018) 2153–2183. <https://doi.org/10.1177/1528083716654468>.
- [21] A. Bessadok, S. Marais, F. Gouanvé, L. Colasse, I. Zimmerlin, S. Roudesli, M. Métayer, Effect of chemical treatments of Alfa (*Stipa tenacissima*) fibres on water-sorption properties, *Compos. Sci. Technol.* 67 (2007) 685–697. <https://doi.org/10.1016/j.compscitech.2006.04.013>.
- [22] Y. Han, S.O. Manolach, F. Denes, R.M. Rowell, Cold plasma treatment on starch foam reinforced with wood fiber for its surface hydrophobicity, *Carbohydr. Polym.* 86 (2011) 1031–1037. <https://doi.org/10.1016/j.carbpol.2011.05.056>.
- [23] X. Li, L.G. Tabil, S. Panigrahi, Chemical Treatments of Natural Fiber for Use in Natural Fiber-Reinforced Composites: A Review, *J. Polym. Environ.* 15 (2007) 25–33. <https://doi.org/10.1007/s10924-006-0042-3>.
- [24] O. Faruk, A.K. Bledzki, H.-P. Fink, M. Sain, Biocomposites reinforced with natural fibers: 2000–2010, *Prog. Polym. Sci.* 37 (2012) 1552–1596. <https://doi.org/10.1016/j.progpolymsci.2012.04.003>.
- [25] M.N. Ichazo, C. Albano, J. Gonza, Polypropylene/wood flour composites: treatments and properties, *Compos. Struct.* 54 (2001) 207–214. [https://doi.org/10.1016/S0263-8223\(01\)00089-7](https://doi.org/10.1016/S0263-8223(01)00089-7).
- [26] A. Hassan, N.Abd. Rahman, R. Yahya, Extrusion and injection-molding of glass fiber/MAPP/polypropylene: effect of coupling agent on DSC, DMA, and mechanical properties, *J. Reinf. Plast. Compos.* 30 (2011) 1223–1232. <https://doi.org/10.1177/0731684411417916>.
- [27] B. Mohebbi, P. Fallah-Moghadam, A.R. Ghotbifar, S. Kazemi-Najafi, Influence of Maleic-Anhydride-Polypropylene (MAPP) on Wettability of Polypropylene/Wood Flour/Glass Fiber Hybrid Composites, *J. Agr. Sci. Tech.* 13 (2011) 877–884.
- [28] M. Pouzet, M. Dubois, K. Charlet, A. Béakou, From hydrophilic to hydrophobic wood using direct fluorination: A localized treatment, *C. R. Chim.* 21 (2018) 800–807. <https://doi.org/10.1016/j.crci.2018.03.009>.
- [29] Z. Cheng, B. Li, J. Huang, T. Chen, Y. Liu, X. Wang, X. Liu, Covalent modification of Aramid fibers' surface via direct fluorination to enhance composite interfacial properties, *Mater. Des.* 106 (2016) 216–225. <http://dx.doi.org/10.1016/j.matdes.2016.05.120>.
- [30] A.P. Kharitonov, R. Taege, G. Ferrier, V.V. Teplyakov, D.A. Syrtsova, G.-H. Koops, Direct fluorination—Useful tool to enhance commercial properties of

- polymer articles, *J. Fluor. Chem.* 126 (2005) 251–263. <https://doi.org/10.1016/j.jfluchem.2005.01.016>.
- [31] A.P. Kharitonov, Practical applications of the direct fluorination of polymers, *J. Fluor. Chem.* 103 (2000) 123–127. [https://doi.org/10.1016/S0022-1139\(99\)00312-7](https://doi.org/10.1016/S0022-1139(99)00312-7).
- [32] M. Pouzet, Modification de l'énergie de surface du bois par fluoration, Thèse en chimie des matériaux, Université Clermont Auvergne, 2017.
- [33] M. Pouzet, M. Dubois, K. Charlet, A. Béakou, The effect of lignin on the reactivity of natural fibres towards molecular fluorine, *Mater. Des.* 120 (2017) 66–74. <http://dx.doi.org/10.1016/j.matdes.2017.01.086>.
- [34] F. Saulnier, Influence de traitements physico-chimiques des renforts sur le comportement mécanique des composites à base de co-produits de bois, Thèse en génie mécanique, Université Blaise Pascal - Clermont II, 2013.
- [35] S.L. Schellbach, S.N. Monteiro, J.W. Drelich, A novel method for contact angle measurements on natural fibers, *Mater. Lett.* 164 (2016) 599–604. <http://dx.doi.org/10.1016/j.matlet.2015.11.039>.
- [36] D.K. Owens, R.C. Wendt, Estimation of the surface free energy of polymers, *J. Appl. Polym. Sci.* 13 (1969) 1741–1747. <https://doi.org/10.1002/app.1969.070130815>.
- [37] A. Roudier, K. Charlet, F. Moreno, E. Toussaint, C. Généau-Sbartai, S. Commereuc, V. Verney, A. Béakou, Caractérisation des propriétés biochimiques et hygroscopiques d'une fibre de lin, *Matér. Tech.* 100 (2012) 525–535. <https://doi.org/10.1051/mattech/2012044>.
- [38] J.-Q. Liu, C. Bai, D.-D. Jia, W.-L. Liu, F.-Y. He, Q.-Z. Liu, J.-S. Yao, X.-Q. Wang, Y.-Z. Wu, Design and fabrication of a novel superhydrophobic surface based on a copolymer of styrene and bisphenol A diglycidyl ether monoacrylate, *RSC Adv.* 4 (2014) 18025–18032. <https://doi.org/10.1039/C4RA01505C>.
- [39] M.G. González, J.C. Cabanelas, J. Baselga, Applications of FTIR on Epoxy Resins - Identification, Monitoring the Curing Process, Phase Separation and Water Uptake, in: T. Theophanides (Ed.), *Infrared Spectroscopy - Materials Science, Engineering and Technology*, InTech, 2012. <https://doi.org/10.5772/36323>.
- [40] J. Huang, X. Nie, A simple and novel method to design flexible and transparent epoxy resin with tunable mechanical properties: Flexible, transparent epoxy resin with tunable mechanical properties, *Polym. Int.* 65 (2016) 835–840. <https://doi.org/10.1002/pi.5144>.
- [41] S. Jiang, S. Zha, L. Xia, R. Guan, Synthesis and characterization of diphenylsilanediol modified epoxy resin and curing agent, *J Adhes Sci Technol.* 29 (2015) 641–656. <https://doi.org/10.1080/01694243.2014.1003177>.
- [42] S.-A. Garea, A.-C. Corbu, C. Deleanu, H. Iovu, Determination of the epoxide equivalent weight (EEW) of epoxy resins with different chemical structure and functionality using GPC and ¹H-NMR, *Polym Test.* 25 (2006) 107–113. <https://doi.org/10.1016/j.polymertesting.2005.09.003>.
- [43] M. Terasaki, T. Kazama, F. Shiraishi, M. Makino, Identification and estrogenic characterization of impurities in commercial bisphenol A diglycidyl ether (BADGE), *Chemosphere.* 65 (2006) 873–880. <https://doi.org/10.1016/j.chemosphere.2006.03.015>.
- [44] W.-H. Lin, R.J. Lagow, The synthesis of highly fluorinated alkylcyclohexanes for use as oxygen carriers and the ¹⁹F and ¹³C NMR spectra of alkylcyclohexanes, *J. Fluor. Chem.* 50 (1990) 345–358.
- [45] R.J. Lagow, J.L. Margrave, Direct Fluorination: A “New” Approach to Fluorine Chemistry, in: S.J. Lippard (Ed.), *Progress in Inorganic Chemistry*, John Wiley &

- Sons, Inc., Hoboken, NJ, USA, 1979: pp. 161–210.
<http://doi.wiley.com/10.1002/9780470166277.ch3>.
- [46] A.P. Kharitonov, *Direct Fluorination of Polymers*, Nova Publishers, 2008.
- [47] A.P. Kharitonov, L.N. Kharitonova, Surface modification of polymers by direct fluorination: A convenient approach to improve commercial properties of polymeric articles, *Pure Appl. Chem.* 81 (2009) 451–471. <https://doi.org/10.1351/PAC-CON-08-06-02>.
- [48] David R. Lide, ed., *CRC Handbook of Chemistry and Physics*, Internet Version 2005, CRC Presse, Boca Raton, FL, 2005.
- [49] V.V. Berenblit, A.Y. Zapevalov, E.S. Panitkova, V.S. Plashkin, D.S. Rondarev, V.P. Sass, S.V. Sokolov, Synthesis and some transformations of perfluoroalkoxy carboxylic acid derivatives, *Zh. Org. Khim.* 15 (1979) 1417–1425.
- [50] W.R. Dolbier, *Guide to fluorine NMR for organic chemists*, 2nd edition, John Wiley & Sons, Inc, Hoboken, New Jersey, 2016.
- [51] A.G. Budnik, T.V. Senchenko, V.D. Shteingarts, Action of electrophilic agents on polyfluoroaromatic compounds. X. Alkylation of 2,3,5,6-tetrafluorophenol, *Zh. Org. Khim.* 10 (1974) 344–350.
- [52] A. Dimitrov, W. Radeck, S. Rudiger, V.E. Platonov, On the electrochemical fluorination of aminoether to give perfluoroamidethers: possible candidates for blood substitutes, *J. Fluor. Chem.* 52 (1991) 317–331. [https://doi.org/10.1016/S0022-1139\(00\)80346-2](https://doi.org/10.1016/S0022-1139(00)80346-2).
- [53] J. Homer, L.F. Thomas, Nuclear magnetic resonance spectra of cyclic fluorocarbons. Part 1.—¹⁹F spectra of fluorocyclohexanes, *Trans. Faraday Soc.* 59 (1963) 2431–2444. <https://doi.org/10.1039/TF9635902431>.
- [54] A. Peake, L.F. Thomas, Nuclear magnetic resonance spectra of cyclic fluorocarbons. Part 2.—F—F and H—F coupling constants in fluorocyclohexanes, *Trans. Faraday Soc.* 62 (1966) 2980–2986. <https://doi.org/10.1039/TF9666202980>.
- [55] V.M. Belous, K.D. Litvinova, L.A. Alekseeva, L.M. Yagupol'skii, Pentafluoroethyl-Substituted phenols and p-Benzoquinones, *Zh. Org. Khim.* 12 (1976) 1798–1802.
- [56] V.A. Grinberg, V.R. Polishchuk, E.I. Mysov, L.S. German, L.S. Kanevskii, Yu.B. Vasil'ev, Anode fluoroalkylation of fluoroolefins, *Izv. Akad. Nauk SSSR, Ser. Khim.* 5 (1979) 988–992. <https://doi.org/10.1007/BF00963312>.
- [57] I.L. Knunyants, YU.A. Cheburkov, N.S. Mirzabekyants, Yu.E. Aronov, Reactions of fluorine-containing ethers, *Izv. Akad. Nauk SSSR, Ser. Khim.* 10 (1972) 2242–2247.
- [58] J.H. Prager, 1,3-Bis(fluoroxy)perfluoropropane and Other Oxygen-Containing Compounds by Direct Fluorination, *J. Org. Chem.* 31 (1966) 392–394. <https://doi.org/10.1021/jo01340a010>.
- [59] M. Kol, S. Rozen, E. Appelman, Isolation and characterization of methyl hypofluorite (CH₃OF), *J. Am. Chem. Soc.* 113 (1991) 2648–2651. <https://doi.org/10.1021/ja00007a043>.
- [60] L. Luo, P. Wu, Z. Cheng, D. Hong, B. Li, X. Wang, X. Liu, Direct fluorination of para-aramid fibers 1: Fluorination reaction process of PPTA fiber, *J. Fluor. Chem.* 186 (2016) 12–18. <https://doi.org/10.1016/j.jfluchem.2016.04.002>.
- [61] J. Maity, C. Jacob, C.K. Das, R.P. Singh, Direct fluorination of Twaron fiber and investigation of mechanical thermal and morphological properties of high density polyethylene and Twaron fiber composites, *J. Appl. Polym. Sci.* 107 (2008) 3739–3749. <https://doi.org/10.1002/app.27510>.
- [62] J. Maity, C. Jacob, C.K. Das, S. Alam, R.P. Singh, Direct fluorination of UHMWPE fiber and preparation of fluorinated and non-fluorinated fiber

- composites with LDPE matrix, *Polym Test.* 27 (2008) 581–590. <https://doi.org/10.1016/j.polymertesting.2008.03.001>.
- [63] A.P. Kharitonov, G.V. Simbirtseva, A. Tressaud, E. Durand, C. Labrugère, M. Dubois, Comparison of the surface modifications of polymers induced by direct fluorination and rf-plasma using fluorinated gases, *J. Fluor. Chem.* 165 (2014) 49–60. <https://doi.org/10.1016/j.jfluchem.2014.05.002>.
- [64] L. Luo, D. Hong, L. Zhang, Z. Cheng, X. Liu, Surface modification of PBO fibers by direct fluorination and corresponding chemical reaction mechanism, *Compos. Sci. Technol.* 165 (2018) 106–114. <https://doi.org/10.1016/j.compscitech.2018.06.014>.
- [65] Z. Yoshimitsu, A. Nakajima, T. Watanabe, K. Hashimoto, Effects of Surface Structure on the Hydrophobicity and Sliding Behavior of Water Droplets, *Langmuir.* 18 (2002) 5818–5822. <https://doi.org/10.1021/la020088p>.
- [66] K. Charlet, C. Baley, C. Morvan, J.P. Jernot, M. Gomina, J. Bréard, Characteristics of Hermès flax fibres as a function of their location in the stem and properties of the derived unidirectional composites, *Compos. Part A: Appl. Sci. Manuf.* 38 (2007) 1912–1921. <https://doi.org/10.1016/j.compositesa.2007.03.006>.